

Multi-scale tests of independence powerful for detecting explicit or implicit functional relationship

Angshuman Roy¹ and Sagnik Das²

¹Department of Mathematics and Statistics, Indian Institute of Technology, Tirupati

²Indian Institute of Science Education and Research, Kolkata

Abstract

In this article, we consider the problem of testing the independence between two random variables. Our primary objective is to develop tests that are highly effective at detecting associations arising from explicit or implicit functional relationship between two variables. We adopt a multi-scale approach by analyzing neighborhoods of varying sizes within the dataset and aggregating the results. We introduce a general testing framework designed to enhance the power of existing independence tests to achieve our objective. Additionally, we propose a novel test method that is powerful as well as computationally efficient. The performance of these tests is compared with existing methods using various simulated datasets.

1 Introduction

Tests of independence play a vital role in statistical analysis. They are used to determine relationships between variables, validate models, select relevant features from a large pool of features, and establish causal directions, among other applications. These tests are particularly important in fields such as economics, biology, social sciences, and clinical trials.

The mathematical formulation for testing independence is as follows. Consider two random variables X and Y with distribution functions F_X and F_Y , respectively, and let F represent their joint distribution function. The objective is to test the null hypothesis H_0 against the alternative hypothesis H_1 based on n independent and identically distributed (i.i.d.) observations $(x_1, y_1), (x_2, y_2), \dots, (x_n, y_n)$ drawn from F , where

$$\begin{cases} H_0 : F = F_X F_Y \\ H_1 : F \neq F_X F_Y. \end{cases} \quad (1)$$

A substantial amount of research has been conducted on this topic, and it remains an active area of investigation. Pearson’s correlation is perhaps the most well-known classical measure that quantifies linear dependence. Spearman’s rank correlation [Spearman, 1904] and Kendall’s concordance-discordance statistic [Kendall, 1938] are used to measure monotonic associations. Hoeffding [1948] proposed a measure using the L_2 distance between the joint distribution function and the product of marginals. Székely et al. [2007] introduced distance correlation (dCor), based on energy distance, while Gretton et al. [2007] leveraged kernel methods to develop the Hilbert-Schmidt independence criterion (HSIC). Reshef et al. [2011] proposed the maximal information coefficient (MIC), an information-theoretic measure that reaches its maximum when one variable is a function of the other. [Heller et al., 2013] introduced a powerful test that breaks down the problem into multiple 2×2 contingency table independence tests and aggregates the results. Zhang [2019] proposed a test that is uniformly consistent with respect to total variation distance. Roy et al. [2020], and Roy [2020] used copula and checkerboard copula approaches to propose monotonic transformation-invariant tests of dependence for two or more variables. Chatterjee [2021] introduced an asymmetric measure of dependence with a simple form and an asymptotic normal distribution under independence, which attains its highest value only when a functional relationship exists. These are just a few of the many contributions in this field.

Different tests of independence have unique strengths and limitations. As demonstrated in Theorem 2.2 of Zhang [2019], no test of independence can achieve uniform consistency. This implies that for any fixed sample size, the power of a test cannot always exceed the nominal level across all alternatives. Therefore, selecting the most appropriate test for a given scenario is crucial. For instance, the correlation coefficient is particularly powerful for detecting dependence between two jointly normally distributed random variables. It is highly effective at identifying linear relationships. Similarly, Spearman’s rank correlation is particularly suited for detecting monotonic relationships.

In this article, we aim to develop tests of independence (as described in Equation 1) that will be particularly powerful for detecting association between two random variables, X and Y , that adhere to the following parametric equation:

$$\begin{cases} X = f(Z) + \epsilon_X \\ Y = g(Z) + \epsilon_Y, \end{cases} \quad (2)$$

where f and g are continuous functions not constant on any interval, Z is a continuous random variable defined on an interval, and ϵ_X and ϵ_Y are independent noise components that are each independent of Z . As a result, our tests will also be powerful for detecting association between random variables X and Y that are functionally related to each other, i.e., when $Y = f(X) + \epsilon_Y$ or $X = g(Y) + \epsilon_X$. In contrast to the method proposed by Chatterjee [2021], which is powerful for detecting dependence when Y is a function of X , in our approach, X and Y are treated symmetrically.

The article is organized as follows. In Section 2, we introduce a general test-

ing framework aimed at enhancing the power of existing tests of independence in scenarios described by Equation (2) and examine its computational complexity. In Section 3, we apply this framework to develop a novel test of independence and analyze its computational complexity. Section 4 presents a performance comparison of our methods on various simulated datasets. Finally, we conclude with a discussion and summary of our findings.

2 A General Testing Framework

Let us begin this section with a few examples of continuous dependent random variables X and Y that satisfy the parametric equation described in Equation 2. We consider three examples, referred to as Example A, B, and C.

- Example A: $X = \Theta + \epsilon_X$ and $Y = \sin(\Theta) + \epsilon_Y$, where Θ , ϵ_X , and ϵ_Y are mutually independent, with $\Theta \sim U(0, 2\pi)$ and $\epsilon_X, \epsilon_Y \sim N(0, (1/20)^2)$.
- Example B: $X = \cos(\Theta) + \epsilon_X$ and $Y = \sin(\Theta) + \epsilon_Y$.
- Example C: $Y = U + \epsilon_Y$ and $X = U^2 + \epsilon_X$, where $U \sim U(0, 1)$ and U is independent of ϵ_X and ϵ_Y .

The scatter plots for these examples are shown in Figure 1. A common feature of all these examples is that within certain neighborhoods around support points, the conditional correlation between X and Y is non-zero. Specifically, there exist points (x_0, y_0) and (x', y') in the support of the distribution such that $\text{Cor}(X, Y \mid (X, Y) \in N(x, y; |x' - x_0|, |y' - y_0|))$ is non-zero, where $N(x, y; \epsilon_1, \epsilon_2)$ represents the ϵ_1, ϵ_2 -neighborhood of (x, y) , defined as $[x - \epsilon_1, x + \epsilon_1] \times [y - \epsilon_2, y + \epsilon_2]$. In Figure 1, red rectangles highlight instances of such neighborhoods with non-zero conditional correlation.

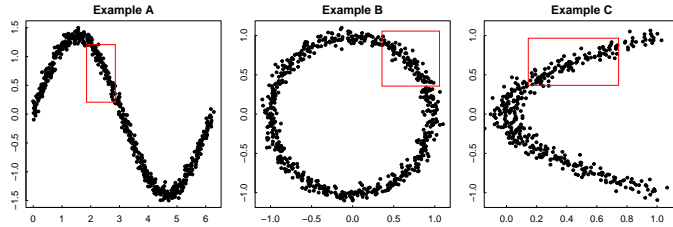


Figure 1: Neighborhoods having non-zero conditional correlation in Example A, B, and C.

As the next example, we consider the BEX_d distribution, originally introduced in [Zhang, 2019] where it is defined as the uniform distribution over a set of parallel and intersecting lines given by $\sum_{i=1}^{2^d-1} \sum_{j=1}^{2^d-1} (|x - c_i| - |y - c_j|) I[|x - c_i| \leq 2^{-d}, |y - c_j| \leq 2^{-d}] = 0$, where $c_i = (2i - 1)/2^d$. Figure 2 illustrates the BEX_d distribution for $d = 2, 3$, and 4. If (X, Y) follows the BEX_d distribution, the

marginals X and Y are dependent but both follow a continuous uniform distribution over $[0, 1]$. Moreover, X and Y can be shown to satisfy Equation 2. Although $\text{Cor}(X, Y) = 0$ for the BEX_d distribution, there exist neighborhoods around support points where the conditional correlation is extremely high. Red

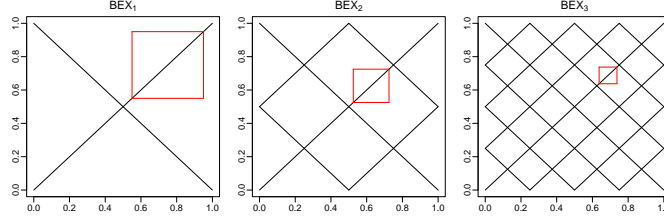


Figure 2: Existence of neighborhoods having high conditional correlation values in BEX_d distributions.

rectangles highlight some such neighborhoods with high conditional correlation values in BEX_1 , BEX_2 , and BEX_3 distributions in Figure 2.

These examples suggest that by calculating the test statistics for an existing test of independence across different neighborhoods and aggregating these values meaningfully, we can enhance its power, especially in scenarios described by Equation (2). Building on this idea, we introduce a multi-scale approach for existing tests of independence in this section.

Let $\mathbf{xy}_{1:n}$ denote the n i.i.d. observations $(x_1, y_1), \dots, (x_n, y_n)$. We analyze the dataset using neighborhoods of varying sizes centered at each observation point, with the distances from the center point to other observations serving as our guide for selecting neighborhood sizes. For a given sample $\mathbf{xy}_{1:n}$ from a bivariate distribution F , we consider all neighborhoods of the form $N(x_i, y_i; |x_j - x_i|, |y_j - y_i|)$ for $i \neq j$. Thus, we consider a total of $n(n-1)$ neighborhoods. For notational convenience, we denote $N(x_i, y_i; |x_j - x_i|, |y_j - y_i|)$ by $N_{i,j}$.

Let T be a test statistic for testing independence between two univariate random variables. Let us use the notation $T(\mathbf{xy}_{1:n})$ to denote the value of the test statistic T computed on the sample $\mathbf{xy}_{1:n}$. Here, we consider only those test statistics T such that $T(\mathbf{xy}_{1:n}) \geq 0$, $T(\mathbf{xy}_{1:n}) \rightarrow 0$ in probability as $n \rightarrow \infty$ under independence, and the rejection region is of the form $\{T(\mathbf{xy}_{1:n}) > C_n\}$ for some constant $C_n > 0$. For example, Person's correlation coefficient cannot be considered as T , but its absolute value can be used. We define $T_{i,j} := T(\mathbf{xy}_{1:n} \cap N_{i,j})$, that is, $T_{i,j}$ is the value of the test statistic T when evaluated on the observations that fall within the neighborhood $N_{i,j}$. If T is undefined on $\mathbf{xy}_{1:n} \cap N_{i,j}$ (it may happen when $x_i = x_j$ or $y_i = y_j$), we set $T_{i,j} := 0$. One naive way to aggregate all the findings from different neighborhoods is to sum $T_{i,j}$'s, that is, to consider $\sum_{1 \leq i \neq j \leq n} T_{i,j}$ as our test statistics. The problem with this summation is that if the dependency information is limited to relatively small neighborhoods, summing all the $T_{i,j}$ values might introduce noise into this information. To address this issue, we separate $T_{i,j}$'s in $(n-1)$ distinct groups

according to the proximity between (x_i, y_i) and (x_j, y_j) . A detailed description is as follows.

For each observation (x_i, y_i) , we order remaining observations according to their Euclidean distance from (x_i, y_i) . Random tie-breaking is to be used in case of ties while ordering. Let $(x_{\pi_i(1)}, y_{\pi_i(1)}), \dots, (x_{\pi_i(n-1)}, y_{\pi_i(n-1)})$ be the observations ordered by their Euclidean distance from (x_i, y_i) in ascending order. Thus, $N_{i, \pi_i(k)}$ is the neighborhood of (x_i, y_i) that has k -th nearest neighbor of (x_i, y_i) at one of its vertices. It is easy to see that for a fixed i , the length of the diagonal of $N_{i, \pi_i(k)}$ increases as k increases. We average the value of the test statistic T based on the sample $\mathbf{xy}_{1:n} \cap N_{i, \pi_i(k)}$ keeping k fixed and varying over i over $1, \dots, n$. We denote this average as $T_{[k]}$, that is, $T_{[k]} := n^{-1} \sum_{i=1}^n T(\mathbf{xy}_{1:n} \cap N_{i, \pi_i(k)}) = n^{-1} \sum_{i=1}^n T_{i, \pi_i(k)}$. To determine how extreme the value of $T_{[k]}$ is, we need to know its distribution under the independence of the marginals, which can be estimated by resampling technique. We discuss this in details next.

Given a sample $\mathbf{xy}_{1:n}$, a randomly permuted sample $\mathbf{xy}_{1:n}^{(\tau)}$ can be generated, where $\tau(1), \dots, \tau(n)$ is a random permutation of $1, \dots, n$ and $\mathbf{xy}_{1:n}^{(\tau)} := \{(x_1, y_{\tau(1)}), \dots, (x_n, y_{\tau(n)})\}$. We calculate $T_{[1]}, \dots, T_{[n-1]}$ in the same way on the sample $\mathbf{xy}_{1:n}^{(\tau)}$ and denote their values with $T_{[1]}^{(\tau)}, \dots, T_{[n-1]}^{(\tau)}$. For B independent random permutations τ_1, \dots, τ_B , we can compute $T_{[k]}^{(\tau_1)}, \dots, T_{[k]}^{(\tau_B)}$ for $1 \leq k \leq n-1$. According to the permutation test principle, the empirical distribution of $T_{[k]}^{(\tau_1)}, \dots, T_{[k]}^{(\tau_B)}$ is an estimator of the distribution of $T_{[k]}$ under independence. We can estimate the mean of $T_{[k]}$ under independence by $\bar{T}_{[k]}^{H_0} := B^{-1} \sum_{i=1}^B T_{[k]}^{(\tau_i)}$ and the standard deviation of $T_{[k]}$ under independence by $s_{[k]}^{H_0} := \sqrt{B^{-1} \sum_{i=1}^B (T_{[k]}^{(\tau_i)} - \bar{T}_{[k]}^{H_0})^2}$. Next we compute Z-score of $T_{[k]}$ with respect to its distribution under independence by $z_k := \frac{T_{[k]} - \bar{T}_{[k]}^{H_0}}{s_{[k]}^{H_0}}$. If $s_{[k]}^{H_0} = 0$, we define $z_k = 0$. The Z-scores z_1, \dots, z_{n-1} suggest how extreme the values of $T_{[1]}, \dots, T_{[n-1]}$ are. Analyzing them for a sample $\mathbf{xy}_{1:n}$ can give us valuable insight into the dependence structure. We demonstrate this point below using various bivariate distributions.

In this illustration, we consider two popular test statistics as T : absolute value of Pearson's correlation and distance correlation. We denote these two test statistics by T^{cor} and T^{dcor} respectively. We consider eight bivariate distributions, description of each is provided in the Table 1. The scatter plots of these distributions are presented in Figure 3. It is easy to see that except for the 'Square' distribution, X and Y are dependent in all the other distributions.

From each distribution, we generated 50 i.i.d. observations and calculated z_1, \dots, z_{49} . By repeating this step independently 1000 times, we then calculated the average values $\bar{z}_1, \dots, \bar{z}_{49}$. We plotted these average values for each distribution in Figure 4. Under independence, it is evident that the expected value of z_k is 0. Therefore, if z_k deviates from 0, it will be indicative of dependence.

From Figure 4, we observe that the average Z-score values are close to 0

Distribution	Description
(a) Square	$X, Y \stackrel{\text{i.i.d.}}{\sim} U(-1, 1)$
(b) Straight line	$X \sim U(-1, 1), Y = X$
(c) Noisy straight line	$U \sim U(-1, 1), X = U + e_X, Y = U + e_Y,$ $e_X, e_Y \stackrel{\text{i.i.d.}}{\sim} N(0, 0.1)$
(d) Sine	$X \sim U(0, 2\pi), Y = \sin(5X),$
(e) Circle	$\Theta \sim U(0, 2\pi), X = \cos(\Theta), Y = \sin(\Theta)$
(f) Noisy parabola	$U \sim U(-1, 1), X = U^2 + \epsilon_X, Y = U + \epsilon_Y,$ $e_X, e_Y \stackrel{\text{i.i.d.}}{\sim} N(0, 0.25)$
(g) BEX_2	As described in Section 1
(h) BVN, rho=0.5	(X, Y) follows bivariate normal distribution with zero means, unit variances and correlation coefficient 0.5

Table 1: Description of distributions considered

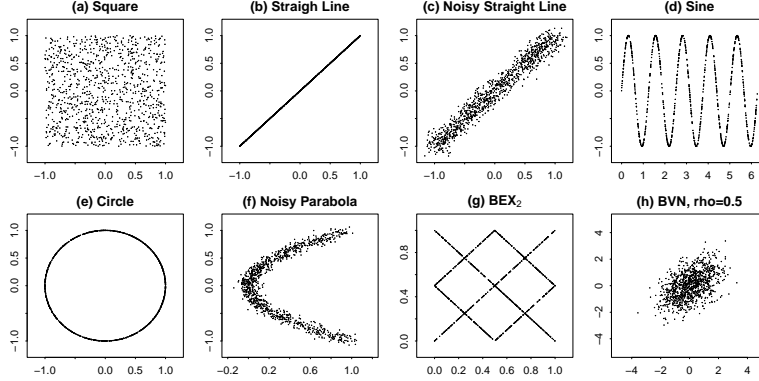


Figure 3: Scatter plots of different datasets used

for ‘Square’ distribution as X and Y are independent. For the ‘Straight line’ and ‘Noisy straight line’ distributions, the average Z-scores are higher in larger neighborhoods for both T^{cor} and T^{dcor} . However, in the ‘Noisy straight line’, the dependence information is less apparent in smaller neighborhoods compared to the ‘Straight line’. For the ‘Sine’ distribution, the dependence information is clearly noticeable in smaller neighborhoods. An interesting phenomenon occurs with the ‘Circle’ distribution, where most neighborhoods, including the largest ones, contain arcs, allowing both T^{cor} and T^{dcor} to detect dependence effectively in most neighborhoods. In the ‘Noisy parabola’, the dependence is most prominent in mid-sized neighborhoods. For the more complex BEX_2 distribution, these statistics detect the dependence patterns in smaller and mid-sized neighborhoods, but less so in larger ones. Finally, in ‘BVN, rho=0.5’, the dependence information is only clearly evident in larger neighborhoods.

It follows clearly from the above illustration that test statistics such as absolute value of correlation and distance correlation sometimes detect dependence

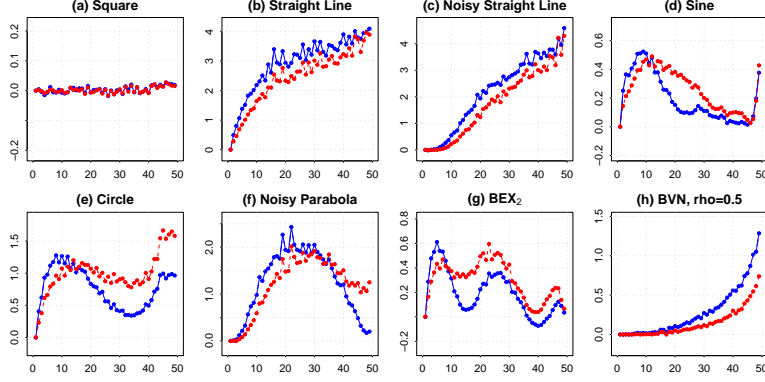


Figure 4: The plot of $\bar{z}_1, \dots, \bar{z}_{49}$ for different distributions. The blue and red points are corresponding to T^{cor} and T^{dcor} statistics respectively.

information better in smaller neighborhoods, sometimes in mid-sized, and sometimes in larger neighborhoods. Therefore, it makes sense to aggregate information from all the Z-scores z_1, \dots, z_{n-1} . We propose an aggregation method in the following paragraph.

First, we observe that under independence, the expected value of z_k is 0 for $k = 1, \dots, n-1$. Under dependence, if the $T_{i,j}$'s are stochastically larger, $T_{[k]}$ will also be stochastically larger. In that case, the expected values of z_k will also be positive. Let μ_k be the expected value of z_k , that is, $\mu_k = E[z_k]$. Thus testing H_0 against H_1 can be done by testing $H'_0 : \mu_k = 0 \forall k$ vs. $H'_1 : \exists k$ such that $\mu_k > 0$. To test this, we suggest the following test statistic $\Psi_n := \sum_{k=1}^{n-1} (\max\{z_k, 0\})^2$. Clearly, a high value of Ψ_n presents evidence against null hypothesis. To determine the distribution of Ψ_n under H_0 , we again use resampling approach by utilizing B randomly permuted samples $\mathbf{xy}_{1:n}^{(\tau_1)}, \dots, \mathbf{xy}_{1:n}^{(\tau_B)}$ which are already in our disposal. Similar how we computed z_1, \dots, z_{n-1} for $\mathbf{xy}_{1:n}$ using permuted samples $\mathbf{xy}_{1:n}^{(\tau_1)}, \dots, \mathbf{xy}_{1:n}^{(\tau_B)}$, we compute $z_1^{(\tau_i)}, \dots, z_{n-1}^{(\tau_i)}$ for $\mathbf{xy}_{1:n}^{(\tau_i)}$ based on permuted samples $\mathbf{xy}_{1:n}^{(\tau_1)}, \dots, \mathbf{xy}_{1:n}^{(\tau_{i-1})}, \mathbf{xy}_{1:n}^{(\tau_{i+1})}, \mathbf{xy}_{1:n}^{(\tau_B)}$ for $i = 1, \dots, B$. Next we calculate $\Psi_n^{(\tau_i)} := \sum_{k=1}^{n-1} (\max\{z_k^{(\tau_i)}, 0\})^2$ for $i = 1, \dots, B$. Finally we determine the p-value of Ψ_n by $p = B^{-1} \sum_{i=1}^B I[\Psi_n \leq \Psi_n^{(\tau_i)}]$. We reject H_0 if the p-value turns out to be less than the level of significance.

Assume that computing $T(\mathbf{xy}_{1:n})$ requires $\mathcal{O}(\Theta(n))$ operations. In that case, computing $T_{i,j}$ collectively for $1 \leq i \neq j \leq n$ requires $\mathcal{O}(n^2\Theta(n))$ operations. For a fixed $1 \leq i \leq n$, the merge sort algorithm allows us to compute π_i in $\mathcal{O}(n \log n)$ operations. Therefore, determining $T_{[1]}, \dots, T_{[n-1]}$ collectively takes $\mathcal{O}(n^2\Theta(n) + n^2 \log n)$ operations (recall that $T_{[k]} = n^{-1} \sum_{i=1}^n T_{i, \pi_i(k)}$). As a result, the computational complexity of computing z_1, \dots, z_{n-1} together also is $\mathcal{O}(n^2\Theta(n) + n^2 \log n)$ assuming that number of randomly permuted samples B is constant with respect to n . Thus we conclude that $\mathcal{O}(n^2\Theta(n) + n^2 \log n)$ operations are required for computing the test statistics $\Psi_n = \sum_{k=1}^{n-1} (\max\{z_k, 0\})^2$.

Since the correlation coefficient can be calculated in linear time, $\Theta(n) = n$ when $T = T^{cor}$. Thus, the complexity of calculating Ψ_n when $T = T^{cor}$ is $\mathcal{O}(n^3)$. On the other hand, the distance correlation between two univariate random variables can be computed in $\mathcal{O}(n \log n)$ operations [see, Chaudhuri and Hu, 2019]. Therefore, the complexity of calculating Ψ_n when $T = T^{dcor}$ is $\mathcal{O}(n^3 \log n)$.

3 A Special Test Method

In this section, we introduce a testing method that closely follows the framework proposed in the previous section, with a few modifications. X and Y are assumed to be continuous random variables in this setup. The key distinction in this approach lies in the manner in which the $T_{i,j}$ values are computed.

Given a sample $\mathbf{xy}_{1:n}$, we begin by fixing two observations (x_i, y_i) and (x_j, y_j) , where $i \neq j$. Similar to the previous method, we define the neighborhood $N_{i,j} = N(x_i, y_i; |x_j - x_i|, |y_j - y_i|)$, centered at (x_i, y_i) with (x_j, y_j) positioned at a corner of the rectangle defined by the neighborhood. Within this neighborhood, we partition the space into four quadrants, classifying observations according to whether the x -coordinate is less than or greater than x_i and whether the y -coordinate is less than or greater than y_i . Subsequently, a 2×2 contingency table is constructed to count the number of observations in each of these quadrants (see Table 2).

	$x_k < x_i$	$x_k > x_i$
$y_k > y_i$	$a_{i,j}$	$b_{i,j}$
$y_k < y_i$	$c_{i,j}$	$d_{i,j}$

Table 2: Number of (x_k, y_k) that belong to one of the four quadrants of $N_{i,j}$.

Let $a_{i,j}, b_{i,j}, c_{i,j}, d_{i,j}$ represent the frequencies in this contingency table, where $a_{i,j} = \#\{(x_k, y_k) : (x_k, y_k) \in \mathbf{xy}_{1:n} \cap N_{i,j}, x_k < x_i, y_k > y_i\}$, $b_{i,j} = \#\{(x_k, y_k) : (x_k, y_k) \in \mathbf{xy}_{1:n} \cap N_{i,j}, x_k > x_i, y_k > y_i\}$, $c_{i,j} = \#\{(x_k, y_k) : (x_k, y_k) \in \mathbf{xy}_{1:n} \cap N_{i,j}, x_k < x_i, y_k < y_i\}$, and $d_{i,j} = \#\{(x_k, y_k) : (x_k, y_k) \in \mathbf{xy}_{1:n} \cap N_{i,j}, x_k > x_i, y_k < y_i\}$.

$T_{i,j}$ is defined as the absolute value of the phi coefficient calculated from this contingency table:

$$T_{i,j} := \frac{|a_{i,j}d_{i,j} - b_{i,j}c_{i,j}|}{\sqrt{(a_{i,j} + b_{i,j})(c_{i,j} + d_{i,j})(a_{i,j} + c_{i,j})(b_{i,j} + d_{i,j})}}.$$

If $(a_{i,j} + b_{i,j})(c_{i,j} + d_{i,j})(a_{i,j} + c_{i,j})(b_{i,j} + d_{i,j}) = 0$, we set $T_{i,j} = 0$.

Next, we employ the same framework described in the previous section to determine a p-value. For notational convenience, the test statistic T used here will be referred to as T^{phi} .

Following the setup in Figure 4, we plotted the average Z-scores for the T^{phi} statistic across various neighborhood sizes, as shown in Figure 5 to gain a deeper understanding of its underlying mechanism. These values are represented by

red dots. For comparison, the average Z-scores for the T^{cor} statistic are plotted alongside and represented by the blue dots.

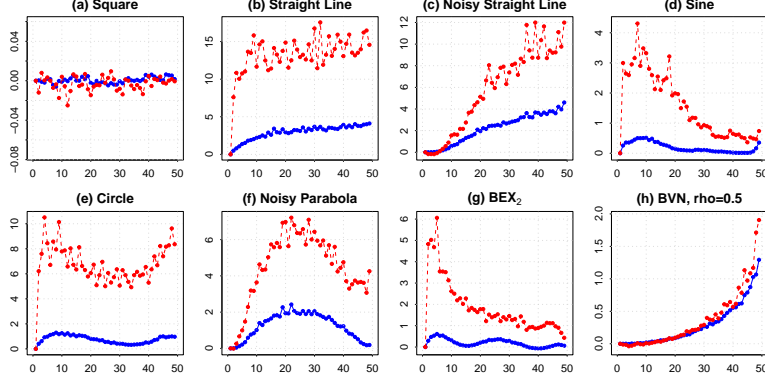


Figure 5: Plot of $\bar{z}_1, \dots, \bar{z}_{49}$ for different distributions. The blue and red points correspond to T^{cor} and T^{phi} statistics, respectively.

As shown in Figure 5(a), the Z-scores for T^{phi} exhibit higher variance compared to T^{cor} under independence. Figures 5(b) through 5(g) demonstrate that T^{phi} consistently yields higher Z-scores than T^{cor} for the ‘Straight line,’ ‘Noisy straight line,’ ‘Sine,’ ‘Circle,’ ‘noisy parabola,’ and ‘ BEX_2 ’ distributions. Additionally, the average Z-score plot for T^{phi} appears to be more wiggly compared to T^{cor} . In the ‘BVN, rho=0.5’ distribution, the average Z-scores of T^{phi} are comparable to those of T^{cor} .

For a fixed $1 \leq i \neq j \leq n$, calculating $T_{i,j}$ requires counting the values $a_{i,j}$, $b_{i,j}$, $c_{i,j}$, and $d_{i,j}$. A straightforward approach to obtain these counts is to check each observation in $\mathbf{xy}_{1:n}$ individually. This process involves $\mathcal{O}(n)$ operations to compute $T_{i,j}$. As established in the previous section, this naive approach requires $\mathcal{O}(n^3)$ operations to compute the test statistics. However, by applying the algorithm described in Lemma 1, which computes $T_{i,j}$ for all $1 \leq j \neq i \leq n$ simultaneously in $\mathcal{O}(n \log n)$ operations for a fixed i , the computational complexity can be significantly reduced. When this algorithm is implemented, calculating $T_{[1]}, \dots, T_{[n-1]}$ collectively will require $\mathcal{O}(n^2 \log n)$ operations. As a result, the complexity of computing the test statistics Ψ_n is reduced to $\mathcal{O}(n^2 \log n)$.

4 Performance on simulated datasets

In this section, we compare the performance of our proposed test methods on various simulated datasets with that of existing tests in the literature. From the proposed general testing framework, we select two well-known test statistics - the absolute value of Pearson’s correlation and distance correlation - as T . We denote the resulting test statistic Ψ_n in these two cases as Ψ_n^{cor} and Ψ_n^{dcor} , re-

spectively. We denote the test statistic Ψ_n for our proposed special test method as Ψ_n^{phi} . As pointed out in previous sections, the computational complexities of Ψ_n^{phi} , Ψ_n^{cor} , and Ψ_n^{dcor} are $\mathcal{O}(n^2 \log n)$, $\mathcal{O}(n^3)$, and $\mathcal{O}(n^3 \log n)$, respectively.

From existing tests of independence, we selected the following popular tests: dCor [Székely et al., 2007], HSIC [Gretton et al., 2007], HHG [Heller et al., 2013], MIC [Reshef et al., 2011], Chatterjee’s correlation (xicor) [Chatterjee, 2021] and BET [Zhang, 2019]. For performing dCor, HSIC, HHG, and xicor tests, we used R packages *energy* [Rizzo and Szekely, 2022], *dHSIC* [Pfister and Peters, 2019], *HHG* [Kaufman et al., 2019], and *XICOR* [Chatterjee and Holmes, 2023], respectively. We calculated the MIC statistic by using ‘mine_stat’ function from the R package *minerva* [Albanese et al., 2012] and subsequently performed a permutation test. For executing BET test, we used the R code provided in the supplemental material of [Zhang, 2019]. We fixed the nominal level at 5%. Except for BET, all other tests were performed using the permutation principle, with the number of permutations set to 1000. The empirical power of a test is determined by calculating the proportion of times it rejects the null hypothesis over 1000 independently generated samples of a specific size from a given distribution.

First, we considered eighty jointly continuous distributions, namely ‘Doppler’, ‘ BEX_2 ’, ‘Lissajous A’, ‘Lissajous B’, ‘Rose curve’, ‘Spiral’, ‘Tilted square’, and ‘Five clouds’. Their descriptions are provided in Table 3. Scatter plots for each of these distributions are presented in Figure 8 in Appendix B. It can be ob-

Distribution	Description
(a) Doppler	$X \sim U(0, 1/2), Y = \sqrt{X} \sin(1/X)$
(b) BEX_2	As described in Section 1
(c) Lissajous A	$\Theta \sim U(0, 2\pi), X = \sin(3\Theta + 3\pi/4) + \epsilon_X, Y = \sin(\Theta) + \epsilon_Y$
(d) Lissajous B	$\Theta \sim U(0, 2\pi), X = \sin(4\Theta + \pi/2) + \epsilon_X, Y = \sin(3\Theta) + \epsilon_Y$
(e) Rose curve	$\Theta \sim U(0, 2\pi), R = \cos(4\Theta), X = R \cos(\Theta) + \epsilon_X/2, Y = R \sin(\Theta) + \epsilon_Y/2$
(f) Spiral	$\Theta \sim U(0, 4\pi), R = \Theta/(2\pi), X = R \cos(\Theta) + \epsilon_X, Y = R \sin(\Theta) + \epsilon_Y$
(g) Tilted Square	$U, V \stackrel{i.i.d.}{\sim} U(-1, 1), X = \cos(\pi/3)U - \sin(\pi/3)V, Y = \sin(\pi/3)U + \cos(\pi/3)V$
(h) Five Clouds	(U, V) uniform on $\{(0, 0), (0, 1), (0.5, 0.5), (1, 0), (1, 1)\}$, $X = U + 2\epsilon_X, Y = V + 2\epsilon_Y$

Table 3: The description of ‘Doppler’, ‘ BEX_2 ’, ‘Lissajous A’, ‘Lissajous B’, ‘Rose curve’, ‘Spiral’, ‘Tilted square’, and ‘Five clouds’ distributions. Here ϵ_X, ϵ_Y are i.i.d. random variables following $N(0, 1/30^2)$, independent of U, V , and Θ .

served from the table that in the ‘Doppler’ distribution, Y is directly a function of X . In ‘Lissajous curve A’, ‘Lissajous curve B’, ‘Rose curve’, and ‘Spiral’, X and Y are related to each other in form of an implicit function. ‘Tilted square’ and ‘five clouds’ are two distributions where X and Y are dependent, but their correlation is 0.

The empirical powers of all test methods on these 8 distributions are presented in Figure 6. It can be seen from this figure that Ψ_n^{phi} performed best in both ‘Doppler’ and ‘ BEX_2 ’ and performed well in all other distributions. Ψ_n^{cor} performed fairly well in all distributions except for ‘Rose curve’ and ‘Tilted square’. Ψ_n^{dcor} performed well in all cases, and in ‘Lissajous curve A’, ‘Lissajous

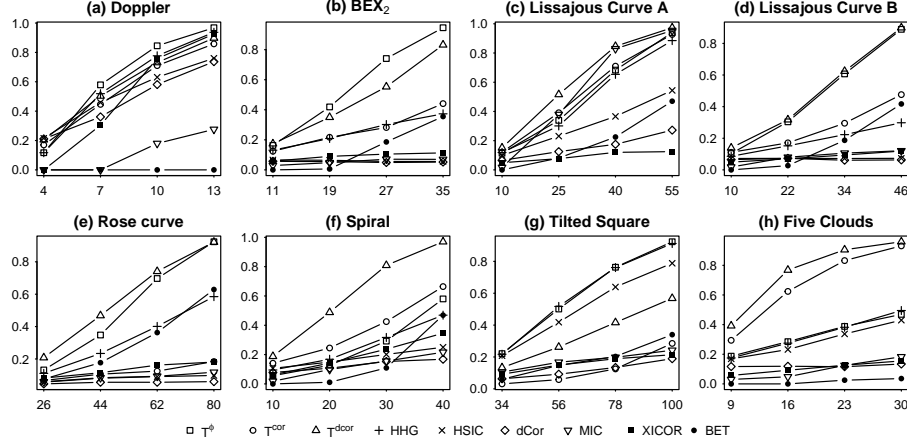


Figure 6: The empirical powers of different test methods on ‘Doppler’, ‘ BEX_2 ’, ‘Lissajous A’, ‘Lissajous B’, ‘Rose curve’, ‘Spiral’, ‘Tilted square’, and ‘Five clouds’.

curve B’, ‘Rose curve’, ‘Spiral’, ‘Five clouds’, it performed the best. HHG yielded satisfactory power overall except for ‘Lissajous curve B’. The power of HSIC is satisfactory only in the ‘Doppler’ and ‘Tilted square’ distributions, not otherwise. dCor, MIC, xicor did not perform well. BET performed somewhat well for larger sample sizes in ‘Lissajous curve B’, ‘Rose curve’ and in ‘Spiral’.

Next, we considered four datasets to assess the performance of our methods under different levels of noise. In these examples, $X = f(Z) + \lambda\epsilon_X$ and $Y = g(Z) + \lambda\epsilon_Y$, where f and g are real functions, Z is a random variable, λ is a non-negative constant, and ϵ_X and ϵ_Y are i.i.d. normal random variables that are also independent of Z . As λ increases, the noise level increases. In particular, we considered 4 distribution named - ‘Parabola λ ’, ‘Circle λ ’, ‘Sine λ ’ and ‘Laminscate λ ’, descriptions of each of these can be found in Table 4. We

Distribution	Description
(a) Parabola λ	$U \sim U(-1, 1), X = U^2 + 2\lambda\epsilon_X, Y = U + 2\lambda\epsilon_Y$
(b) Circle λ	$\Theta \sim U(0, 2\pi), X = \cos(\Theta) + 6\lambda\epsilon_X, Y = \sin(\Theta) + 6\lambda\epsilon_Y$
(c) Sine λ	$\Theta \sim U(0, 2\pi), X = \Theta + 3\lambda\epsilon_X, Y = \sin(\Theta) + 3\lambda\epsilon_Y$
(d) Laminscate λ	$\Theta \sim U(0, 2\pi), X = \frac{\cos(\Theta)}{(1+\sin(\Theta))^2} + 2\lambda\epsilon_X, Y = \frac{\sin(\Theta)\cos(\Theta)}{(1+\sin(\Theta))^2} + 2\lambda\epsilon_Y$

Table 4: The descriptions of ‘Parabola λ ’, ‘Circle λ ’, ‘Sine λ ’ and ‘Laminscate λ ’ distributions. Possible values of lambda are $\lambda = 0, 1, 2$. Here, ϵ_X, ϵ_Y are i.i.d. random variables following $N(0, 1/60^2)$, independent of U and Θ .

considered three noise levels by taking $\lambda = 0, 1, 2$. Scatter plots of the twelve ($4 \times 3 = 12$) distributions are presented in Figure 9 in the Appendix B.

The empirical powers of each of these tests are presented in Figure 7. It can be observed from this figure that Ψ_n^{phi} performs best or next to best in the

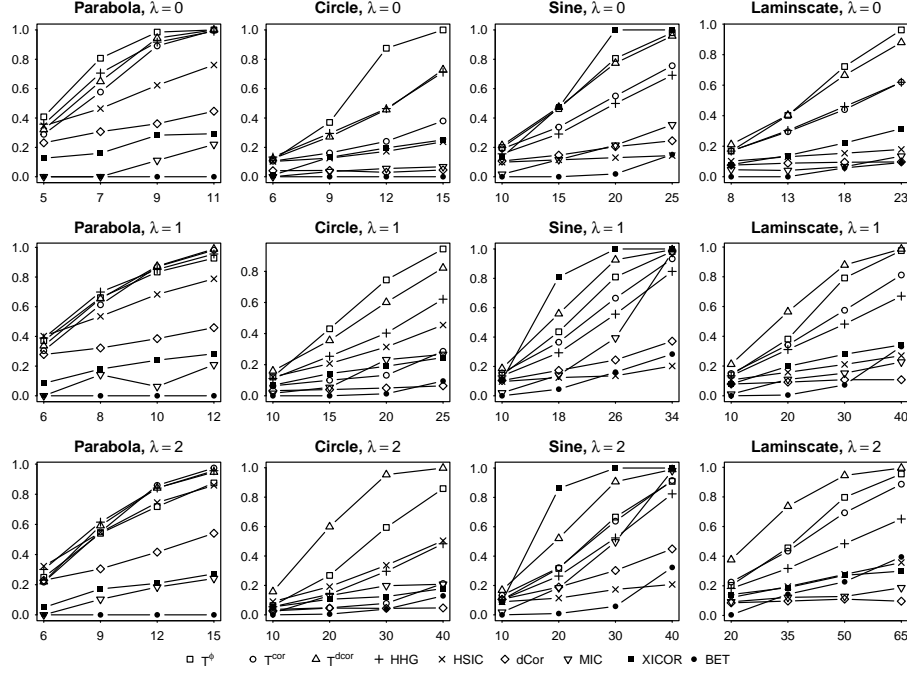


Figure 7: The empirical power of different test methods on ‘parabola λ ’, ‘circle λ ’, ‘sine λ ’ and ‘laminscate λ ’ distributions for $\lambda = 0, 1, 2$.

absence of noise. Even in the presence of noise, power of Ψ_n^{phi} is quite good. As the noise level increases, Ψ_n^{dcor} takes the lead. The overall performance of Ψ_n^{cor} is competitive except for the ‘Circle λ ’ case. HHG performed well but it lagged behind our proposed tests most of the time. HSIC performed well in ‘Parabola λ ’ and ‘Circle λ ’ distributions, but didn’t achieve satisfactory power in other distributions. dCor had a somewhat competitive power in ‘Parabola λ ’, but not in other distributions. MIC had low power overall, except for higher sample sizes in the ‘Sine λ ’ distributions. Xicor also performed poorly except for ‘Sine λ ’, where it performed the best. This is not unexpected from xicor, as it is mainly designed to detect whether Y is a function of X . BET had the lowest power among all tests in most distributions.

5 Discussion and conclusion

We proposed a general framework for testing independence, which can utilize existing independence tests in different neighborhoods of the dataset and combine the results in a meaningful way. This approach has been shown to enhance performance when the variables are explicitly or implicitly functionally dependent. Additionally, we introduced a novel test of independence that leverages

a similar framework. It is important to note that multiple approaches can be taken towards selecting neighborhoods, and both the power and the complexity of the resulting method can vary based on it. Therefore, an optimal selection of neighborhoods could be a potential direction for future research. Our proposed method assigns equal weight to each neighborhood, from nearest to farthest. The potential benefits of using varying weights for different neighborhoods could be explored in future research.

Appendix A

Lemma 1. *For the proposed special test method, for a fixed $1 \leq i \leq n$, the computation of $T_{i,j}$ for all $1 \leq j \neq i \leq n$ can be done collectively in $\mathcal{O}(n \log n)$ operations.*

Proof. Let us fix i such that $1 \leq i \leq n$. At first, we will prove that the sequence $a_{i,1}, \dots, a_{i,i-1}, a_{i,i+1}, \dots, a_{i,n}$ can be computed in $\mathcal{O}(n \log n)$ operations.

For $1 \leq j \neq i \leq n$, $d_j^x = |x_j - x_i|$ and $d_j^y = |y_j - y_i|$ can be computed in $\mathcal{O}(n)$ operations. As $(x_1, y_1), \dots, (x_n, y_n)$ are n i.i.d. observations from a continuous distribution, there are no ties in x -coordinate or in y -coordinate, and hence d_j^x and d_j^y are positive for all $1 \leq j \neq i \leq n$ without any ties.

Using the merge sort algorithm, a permutation ω of the sequence $(1, \dots, i-1, i+1, \dots, n)$ can be computed in $\mathcal{O}(n \log n)$ operations, such that $d_{\omega(1)}^x \leq \dots \leq d_{\omega(i-1)}^x \leq d_{\omega(i+1)}^x \leq \dots \leq d_{\omega(n)}^x$.

Next, by iterating through $j \in \{1, \dots, i-1, i+1, \dots, n\}$ in ascending order, we can store in an array q those j values that satisfy $x_{\omega(j)} < x_i$ and $y_{\omega(j)} > y_i$. As a result, for all $k, l \in \{1, \dots, \text{length}(q)\}$, we have $q[k] < q[l]$ whenever $k < l$, with $x_{\omega(q[k])} < x_i$ and $y_{\omega(q[k])} > y_i$. The remaining integers in $\{1, \dots, i-1, i+1, \dots, n\}$ that do not satisfy the conditions for q can be stored in another array r in ascending order. Thus, for all $k, l \in \{1, \dots, \text{length}(r)\}$, we have $r[k] < r[l]$ whenever $k < l$, with $x_{\omega(r[k])} > x_i$ or $y_{\omega(r[k])} < y_i$. This iterative checking and storing process requires only $\mathcal{O}(n)$ operations. Note that q and r have no common elements, and together they contain all elements from the set $\{1, \dots, i-1, i+1, \dots, n\}$.

Given an array of real numbers $[s_1, \dots, s_m]$, the ‘surpasser count’ is defined as an array of integers $[t_1, \dots, t_m]$ of the same length, where $t_j = \sum_{k=j+1}^m I[s_j < s_k]$ for $1 \leq j \leq m$. Using the merge sort technique, this can be computed in $\mathcal{O}(m \log m)$ operations [see Bird, 2010, Chapter 2]. Instead of using the surpasser count algorithm directly, we’ll use the ‘trail count’. For a given array of real numbers $[s_1, \dots, s_m]$, the trail count is defined as an array of integers $[t_1, \dots, t_m]$ of the same length, where $t_j = \sum_{k=1}^j I[s_j \geq s_k] = 1 + \sum_{k=1}^{j-1} I[s_j > s_k]$ for $1 \leq j \leq m$. Essentially, the trail count is the surpasser count applied to the reversed array, thus maintaining the same complexity.

We apply the trail count to the array $[d_{\omega(1)}^y, \dots, d_{\omega(i-1)}^y, d_{\omega(i+1)}^y, \dots, d_{\omega(n)}^y]$, resulting in the array, say, $[w_1, \dots, w_{i-1}, w_{i+1}, \dots, w_n]$. It’s easy to verify that w_k represents the number of observations, excluding (x_i, y_i) , that are within the

neighborhood $N_{i,\omega(k)}$ for $1 \leq k \neq i \leq n$. Next, we apply the trail count to the array $[d_{\omega(q[1])}^y, \dots, d_{\omega(q[\text{length}(q)])}^y]$, resulting in the array, say, $[u_1, \dots, u_{\text{length}(q)}]$. It can be verified that u_k is the number of observations that fall within the set $\{(x, y) : (x, y) \in N_{i,\omega(q[k])}, x < x_i, y > y_i\}$ for $1 \leq k \leq \text{length}(q)$. Thus, $a_{i,q[k]} = u_k$ for $1 \leq k \leq \text{length}(q)$. Similarly, applying the trail count to the array $[d_{\omega(r[1])}^y, \dots, d_{\omega(r[\text{length}(r)])}^y]$ results in the array, say, $[v_1, \dots, v_{\text{length}(r)}]$. It can be verified that v_k represents the number of points in the set $\{(x, y) : (x, y) \in N_{i,\omega(r[k])}, x > x_i \text{ or } y < y_i\}$ for $1 \leq k \leq \text{length}(r)$. Therefore, $a_{i,r[k]} = w_{r[k]} - v_k$ for $1 \leq k \leq \text{length}(r)$. Hence, all $a_{i,j}$ for $1 \leq j \neq i \leq n$ can be computed together in $\mathcal{O}(n \log n)$ operations.

Similar steps can be taken to show that for a fixed i , $b_{i,j}, c_{i,j}, d_{i,j}$ for $1 \leq j \neq i \leq n$ can be computed collectively in $\mathcal{O}(n \log n)$ operations. Since $T_{i,j}$ is a function of $a_{i,j}, b_{i,j}, c_{i,j}$, and $d_{i,j}$, it directly follows that computing $T_{i,j}$ collectively for $1 \leq j \neq i \leq n$ also requires $\mathcal{O}(n \log n)$ operations. \square

Appendix B

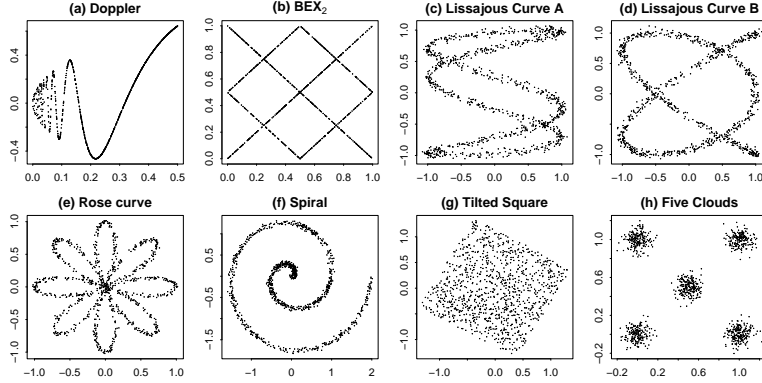


Figure 8: The scatter plots of ‘doppler’, ‘BEX₂’, ‘Lissajous A’, ‘Lissajous B’, ‘rose curve’, ‘spiral’, ‘tilted square’ and ‘five clouds’ distributions.

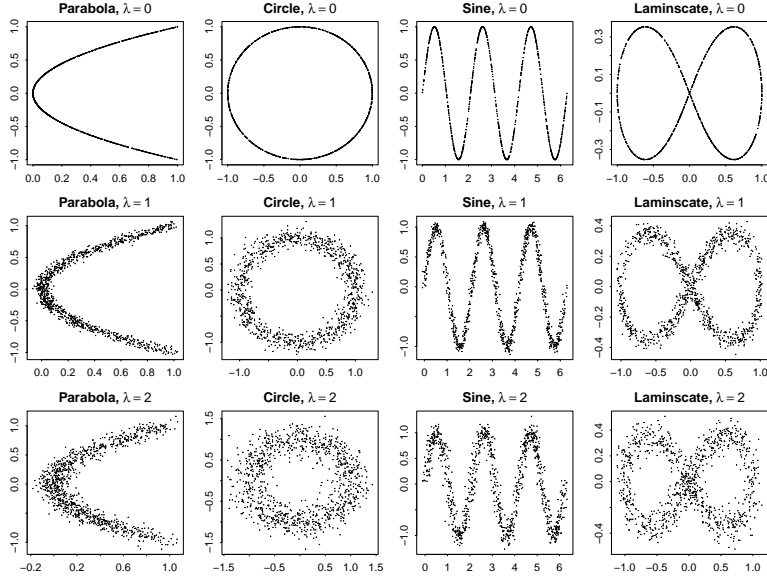


Figure 9: The plot of ‘parabola λ ’, ‘circle λ ’, ‘sine λ ’ and ‘laminscate λ ’ distributions for $\lambda = 0, 1, 2$.

References

- Davide Albanese, Michele Filosi, Roberto Visintainer, Samantha Riccadonna, Giuseppe Jurman, and Cesare Furlanello. Minerva and minepy: a c engine for the mine suite and its r, python and matlab wrappers. *Bioinformatics*, page bts707, 2012.
- Richard Bird. *Pearls of functional algorithm design*. Cambridge University Press, 2010.
- Sourav Chatterjee. A new coefficient of correlation. *Journal of the American Statistical Association*, 116(536):2009–2022, 2021.
- Sourav Chatterjee and Susan Holmes. *XICOR: Robust and generalized correlation coefficients*, 2023. URL <https://CRAN.R-project.org/package=XICOR>. <https://github.com/spholmes/XICOR>.
- Arin Chaudhuri and Wenhao Hu. A fast algorithm for computing distance correlation. *Computational statistics & data analysis*, 135:15–24, 2019.
- Arthur Gretton, Kenji Fukumizu, Choon Teo, Le Song, Bernhard Schölkopf, and Alex Smola. A kernel statistical test of independence. *Advances in neural information processing systems*, 20, 2007.
- Ruth Heller, Yair Heller, and Malka Gorfine. A consistent multivariate test of association based on ranks of distances. *Biometrika*, 100(2):503–510, 2013.

- Wassily Hoeffding. A non-parametric test of independence. *The Annals of Mathematical Statistics*, 19(4):546–557, 1948.
- Barak Brill & Shachar Kaufman, based in part on an earlier implementation by Ruth Heller, and Yair Heller. *HHG: Heller-Heller-Gorfine Tests of Independence and Equality of Distributions*, 2019. URL <https://CRAN.R-project.org/package=HHG>. R package version 2.3.
- Maurice G. Kendall. A new measure of rank correlation. *Biometrika*, 30(1/2): 81–93, 1938.
- Niklas Pfister and Jonas Peters. *dHSIC: Independence Testing via Hilbert Schmidt Independence Criterion*, 2019. URL <https://CRAN.R-project.org/package=dHSIC>. R package version 2.1.
- David N Reshef, Yakir A Reshef, Hilary K Finucane, Sharon R Grossman, Gilean McVean, Peter J Turnbaugh, Eric S Lander, Michael Mitzenmacher, and Pardis C Sabeti. Detecting novel associations in large data sets. *science*, 334(6062):1518–1524, 2011.
- Maria Rizzo and Gabor Székely. *energy: E-Statistics: Multivariate Inference via the Energy of Data*, 2022. URL <https://CRAN.R-project.org/package=energy>. R package version 1.7-11.
- Angshuman Roy. Some copula-based tests of independence among several random variables having arbitrary probability distributions. *Stat*, 9(1):e263, 2020.
- Angshuman Roy, Anil K Ghosh, Alok Goswami, and CA Murthy. Some new copula based distribution-free tests of independence among several random variables. *Sankhya A*, pages 1–41, 2020.
- Charles Spearman. The proof and measurement of association between two things. *The American Journal of Psychology*, 15(1):72–101, 1904.
- Gábor J Székely, Maria L Rizzo, and Nail K Bakirov. Measuring and testing dependence by correlation of distances. *The Annals of Statistics*, 35(6):2769–2794, 2007.
- Kai Zhang. Bet on independence. *Journal of the American Statistical Association*, 2019.